Multi-angular radiances of an isolated convective cloud: comparison between MISR measurements and Monte-Carlo simulation

C. Cornet[1] and R. Davies[2]

(1) Laboratoire d'Optique Atmosphérique, Université de Lille, France
(2) Department of Physics, The University of Auckland, New Zealand

1. Introduction

Deep convective clouds play an important role in the hydrological cycle because they often have large vertical extents and so contain large amounts of liquid water. In the context of climate change, it is then crucial to be able to look at their evolution. The most practical way of accomplishing this task globally is by satellite observation. However, for practical reasons, current cloud retrieval algorithms use the assumption of a homogeneous cloud with infinite horizontal extent. This assumption has often been questioned because of the errors caused by cloud heterogeneity such as brightness and shadowing effects or smoothing of the radiances fields. In case of deep convective cloud, these heterogeneity effects common to all clouds are present and can even be stronger. But additionally, due to their finite dimensions and their high vertical extent, photons escape by the cloud sides and because of their large liquid water content, the 1-D radiances usually reach their saturation limit. That tends to lead to an underestimation of the cloud optical thickness.

In this study, the reconstruction of a convective cloud obtained from the measurements of the Multiangle Imaging SpectroRadiometer MISR is used to simulate the 3D radiative transfer inside the cloud. We take advantage of these simulations to assess the optical thickness errors made with the one dimensional radiative transfer theory.

2. Case description

We used data from the MISR instrument on the Terra spacecraft. The instrument looks at the Earth with nine cameras with viewing zenith angle of 0° (An); ± 26.1° (Af, Aa); ± 45.6° (Bf, Ba); ± 60° (Cf, Ca) and ± 70.5° (Df, Da). The time delay between the first camera and the last camera is seven minutes which enable us to assume, in the following, that the cloud had not moved between the measurement by the first and the last camera. The instrument possessed four spectral bands but we will use only the red band (0.672μm) which is registered with the highest resolution of 275m.

For this study, we selected an isolated convective cloud above the Pacific Ocean. The MISR measurements were acquired on 2 September 2003 (path 78). The multi-angularity of the MISR measurement and its high resolution allow us to see the cloud top as well as the cloud sides. In figure 1, the nadir view and the two most oblique views (D camera) are presented. The solar zenith angle is 22.1° and the sun is coming from the right side of the image, almost perpendicularly to the MISR path.

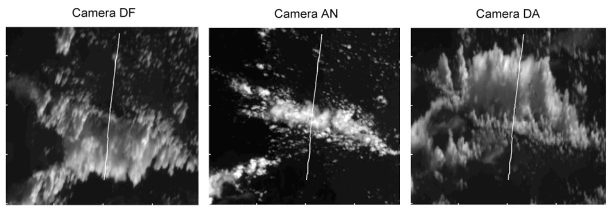

Figure 1: MISR view of the deep convective cloud used for this study. Left: Df Camera (70.5°); center: An camera (0°); right: Da Camera (70.5°)

The white line corresponds to the cross-section where the cloud is reconstructed. This is done with stereographic techniques by using successively the seven pairs of adjacent cameras (Seiz and Davies, 2006). The results are presented in figure 2 (blue dot). Subsequently, from these results, we approximate the cloud contour with the red curve. The vertical extension of the cloud is about 7-8km, with a similar horizontal extent, typical for deep convective clouds.

To be able to compare radiances simulated with a radiative transfer code with radiances measured by MISR, we need to map the radiances along the cloud contour. This is done geometrically by using the cloud-top height obtained from stereo and the information of the zenith and azimuth angles of the camera. In figure 2, the radiances emerging from the cloud in the direction closest to the perpendicular of the cloud envelop are shown. Note that the variation of the radiances is due not only to the cloud geometry, but also to variation in the extinction coefficient.

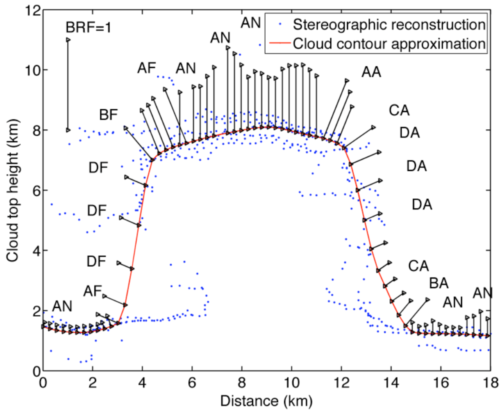

Figure 2: *Blue dot: Stereographic reconstruction of the cloud along the cross-section line in Figure1. Red line: approximation of the cloud contour used for the following radiative transfer calculations. Black Arrow: mapping of the radiances along the cloud contour.*

3. Radiative transfer simulation

The radiative transfer simulation was done with a forward Monte-Carlo code. It uses the classical local estimate method but instead of doing the integration of the optical thickness at each interaction of the photons, the collision density of the photons is stored as a function of position and direction. The integration along the line of sight is done last. That allows substantial savings of computational time (for nine directions we save around a factor 5).

3.1. Clear-sky simulation

Because the scene studied is above the ocean, we cannot assume a Lambertian surface, but need to simulate the anisotropy of the clear sky reflectance. To set the background of our Monte-Carlo simulation, we selected about 200 clear sky pixels around the convective cloud. The red curve in figure 3 represents the mean and the standard deviation of these pixels seen by the nine cameras of MISR. Although the observation angles of the cameras do not correspond exactly to the glitter direction, it is easily distinguishable with the nadir camera. The higher values of the radiances for the C and D cameras are typically due to molecular and aerosols scattering.

To reproduce this clear sky signature, we implement in the Monte-Carlo model the Cox and Munk ocean surface model and add a vertical aerosol and molecular profile. After several iterations, we found that the best match (see figure 3) of the clear-sky measurement is for a wind speed of 2.5 m s^{-1}, a Rayleigh optical thickness of 0.042, and an aerosol optical thickness of 0.09. The latter was ascribed a phase function as used in the operational MISR aerosol retrieval corresponding to a mixture of sea-salt and sulfate.

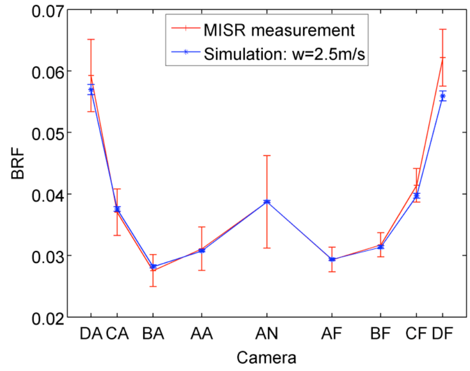

Figure 3: *Mean and standard deviation of the clear-sky radiances measured by the nine cameras of MISR (red). Simulation of these clear-sky radiances with the Monte-Carlo model including the Cox and Munk model and the molecular and aerosol scattering (Blue).*

3.2 Radiative transfer cloud simulation

The radiative transfer calculations of the convective cloud were done by accounting for the cloud morphology described in section 2 and Figure 2 in the X-direction and assuming an infinite cloud in the other direction. Our first hypothesis was to use a constant extinction coefficient and a constant phase function everywhere inside the cloud. We used a C1 phase function and did the calculation for two constant extinction coefficients of 5 km^{-1} and $10km^{-1}$. The computed radiances emerging from the cloud along its contour for the nine cameras are presented respectively in blue and green in figure 4. Note that, except for An, the cameras typically see only one side of the cloud, with the other side being hidden.

This figure shows that just by accounting for the cloud morphology, we can almost capture the general behavior of the radiance fields with an extinction coefficient of $10km^{-1}$, which corresponds in the highest part of the cloud to an optical thickness of 70.

In order to capture the details of the radiance fields, we used the differences between the observed and measured An radiances to adjust the extinction coefficient horizontally. Due to horizontal photon transport and 3D effects of trapping and escape, this approach is not rigorous, but does allow tests of the effects of a variable extinction coefficient.

In red on figure 4, we present our current best results after several iterations. It appears that some adjustments to the sides of the cloud may still be needed. The oblique views of MISR can, for these parts of the cloud, certainly help to improve the results. Concerning the difference in the Ba, Ca, Da cameras, they may also be due to a problem in the mapping of the radiances, as the highest value of the radiances is not in identical locations for the simulation and the observation.

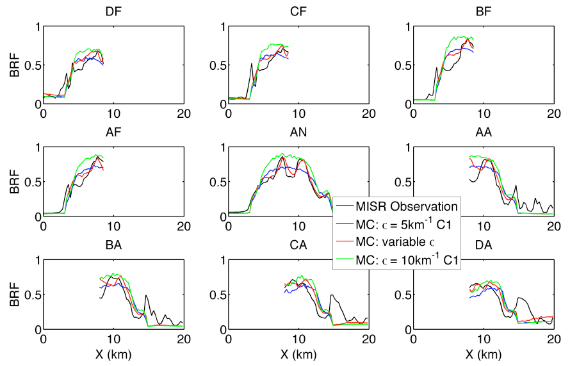

Figure 4: *Comparison of the radiances measured by the nine cameras of MISR (black curves) and simulated by the Monte-Carlo model using the reconstructed cloud contour of Figure 2. In blue and green, for a constant extinction coefficient of 5 km^{-1} and 10km^{-1}. In red, for a variable extinction coefficient.*

However, Figure 4 shows that we almost succeed in matching the behavior of observed radiances for the nine cameras. This result is certainly not unique and tests of the different hypothesis remain to be done (use of a C1 phase function, of a vertically homogeneous extinction coefficient…).

3.3 Optical thickness comparison

Even if the result obtained is not unique, the geometrical thickness and the extinction coefficient of the cloud give us useful information about its optical thickness. We then compared these results with the optical thickness of an infinite homogeneous cloud, usually used in current retrieval algorithms.

As examples, we selected 3 different positions along the cloud contour: 1) around 4km for the side of the cloud; 2) around 9km in the "hole" of the radiances fields and 3) around 11km, in the bump of the radiance fields.

In Figure 5, we plotted the radiances for the nine cameras of an infinite homogeneous cloud with different optical thickness (dashed line). We also plotted the observed (black line) and simulated (red line) radiances for the three selected positions. The optical thicknesses obtained with the 3D calculations are respectively 72, 13 and 158, compared with about 10, 15-20 and 30 for the 1D calculations. In the case 1) and 3) the 1D model significantly underestimates the optical thickness because it does not account for the loss of radiation through the cloud sides. This underestimation is accentuated by the asymptotic shape of the radiances curve versus the optical thickness.

On contrary, in the "hole" (case 2), the optical thickness is almost the same, and even smaller with the 3D simulation: this can be explained by the horizontal transport of the photons from the highest optical thickness part of the cloud to the lowest part which increase the energy in the "hole".

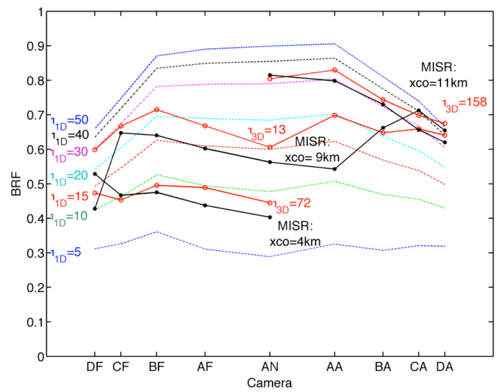

***Figure 5**: Radiances for the nine cameras of MISR obtained under different conditions: computed with the homogeneous assumption for different optical thickness (dashed line); radiances computed accounting for the 3D structure of the cloud (red curves) and MISR measurements (black curves) for different positions along the cloud contour.*

The conclusions obtained from these examples can be applied more generally to the entire cloud contour and certainly to other deep convective clouds.

4. Conclusion

In this study, we used the reconstruction from MISR measurements of the contour of an isolated convective cloud to simulate with a Monte-Carlo model the radiances in the nine directions of MISR. We showed that allowing for cloud morphology and a variable extinction coefficient, 3D radiative transfer simulation is close to reproducing the MISR measurements. We then compared the optical thickness needed to match the MISR radiances with the optical thickness of a homogeneous cloud. We showed that most of the time, the optical thickness retrieved with the 1D theory appears to be significantly underestimated. This can leads to large errors in the liquid water content estimation.

We need, however, to be cautious with these results. Indeed, we use a 2D slice of the cloud and do not account for the variations in the other direction. This assumption seems reasonable regarding the shape of the cloud but shadowing and brightness effects could change these results somewhat.

Moreover, the stereo gives us only the general shape of the cloud but not smallest variation of the geometrical thickness of the cloud. These can modify the amplitude of the results given that geometrical thickness variations have higher effects than optical thickness variations.

5. Acknowledgement

A portion of this work was done while the authors were at the Jet Propulsion Laboratory, California Institute of Technology, under a contract from the National Aeronautics and Space Administration. The data were obtained from the NASA Langley Research Center Atmospheric Sciences Data Center.

6. References

Seiz G. and Davies, R., 2006: Reconstruction of cloud geometry from multi-view satellite images, *Remote Sens. Environ.*, 100, 143-149.